ELSEVIER

Computers in Biology and Medicine 38 (2008) 1045–1055

Computers in Biology and Medicine

www.intl.elsevierhealth.com/journals/cobm

Improvement of microcalcification cluster detection in mammography utilizing image enhancement techniques

A. Papadopoulos[a,b], D.I. Fotiadis[b,*], L. Costaridou[c]

[a]Department of Medical Physics, Medical School, University of Ioannina, GR 45110 Ioannina, Greece
[b]Department of Computer Science, University of Ioannina, Unit of Medical Technology and Intelligent Information Systems, and Biomedical Research Institute—FORTH, GR 45110 Ioannina, Greece
[c]Department of Medical Physics, Medical School, University of Patras, GR 26500 Patras, Greece

Received 10 October 2006; accepted 9 July 2008

Abstract

In this work, the effect of an image enhancement processing stage and the parameter tuning of a computer-aided detection (CAD) system for the detection of microcalcifications in mammograms is assessed. Five (5) image enhancement algorithms were tested introducing the contrast-limited adaptive histogram equalization (CLAHE), the local range modification (LRM) and the redundant discrete wavelet (RDW) linear stretching and shrinkage algorithms. CAD tuning optimization was targeted to the percentage of the most contrasted pixels and the size of the minimum detectable object which could satisfactorily represent a microcalcification. The highest performance in two mammographic datasets, were achieved for LRM ($A_Z = 0.932$) and the wavelet-based linear stretching ($A_Z = 0.926$) methodology.

Keywords: Mammography image enhancement; Preprocessing; Microcalcification detection; CAD

1. Introduction

Mammography is an efficient imaging technique for the detection and diagnosis of breast pathological disorders. During the last decade, mammographic interpretation was assisted by computer-based methods which are used either as visualization tools or as second opinion devices. Visualizing systems operate under experts supervision, aiming at the improvement of mammogram quality and the extraction of substantial information containing critical clinical data. Second opinion schemes, provide useful information indicating probable pathological areas, or even more, characterize the detected abnormality. A computer-aided detection (CAD) system consists of several modules, such as preprocessing, segmentation and classification of pathological cases. In the preprocessing module, the significant features of the mammogram are enhanced, recovering most of the hidden characteristics and improving image quality.

Image enhancement algorithms have been utilized for the improvement of contrast features and the suppression of noise. Initially, contrast enhancement techniques have exploited the convolution function or methodologies such as morphological, edge detection and band-pass filters [1,2]. The enhancement techniques could be classified according to the generalization of their parameters as global, local or adaptive [3,4]. According to the preprocessing algorithms and the type of features which have been reported in literature, during the enhancement procedure specific methodologies were exploited such as: histogram equalization [3,5–7], unsharp masking [5,8,9], region-based [2,10,11], wavelet decomposition [12–17], fractal modeling [18–21] and fuzzy methodology [22–25].

Pizer et al. [3] proposed a methodology based on histogram equalization employing local parameters known as contrast-limited adaptive histogram equalization (CLAHE). Lure et al. [9] proposed an unsharp masking methodology based on high pass and low pass filtered versions of the original images. Morrow et al. [10] proposed a region-based approach for the enhancement of regions of interest (ROIs). The algorithm, named adaptive-neighborhood contrast enhancement, computes a

* Corresponding author. Tel.: +30 2651098819; fax: +30 2651098889.
E-mail address: fotiadis@cs.uoi.gr (D.I. Fotiadis).

0010-4825/$ - see front matter © 2008 Elsevier Ltd. All rights reserved.
doi:10.1016/j.compbiomed.2008.07.006

contrast value for each region utilizing the intensity of foreground and background areas, each one specified by a gray-level deviation. A lookup table is composed enhancing only the areas with low-contrast values.

Wavelets have been also employed in microcalcification detection providing high spatial frequency features in mammograms. Strickland et al. [14] proposed a discrete wavelet transform (DWT) with biorthogonal spline filters. Four dyadic and two additional interpolating scales are extracted by introducing binary thresholds in every scale. Laine et al. [12,26] applied a wavelet-based enhancement methodology utilizing redundant transformation [27,28] and linear/nonlinear mapping functions with Laplacian or gradient wavelet coefficients.

Fractal and fuzzy logic methodologies are also approaches resulting in sophisticated enhancement techniques. Li et al. [18] proposed a fractal modeling scheme. The breast background tissue results in high local self-similarity, but the presence of microcalcifications reduces it. Microcalcifications were enhanced based on the difference between the original and the modeled image. Cheng et al. [25] proposed a fuzzy logic contrast improvement methodology resulting in the enhancement of contours and fine details of the mammographic structures. Local contrast values are improved by the utilization of the maximum fuzzy entropy principle and global information that is extracted by histogram analysis. Jiang et al. [22] applied a fuzzy enhancement operator restructuring the mammograms in fuzzy domain aiming on the detection of microcalcifications. The utilization of maximum fuzzy entropy principle results in the identification of regions with high local fuzzy contrast values which corresponds to microcalcifications.

Various enhancement techniques have been compared in Sivaramakrishna et al. [29] having as evaluation procedure radiologist's scores in clinical soft-copy display settings. Pisano et al. [7] introduce several image processing algorithms improving the contrast of masses in digitized mammograms. Costaridou et al. [30] proposed an enhancement methodology based on wavelet enhancement providing a mammographic enhancement tool for the improvement of radiologist's detection performance.

Mammogram enhancement techniques are utilized to increase radiologist's detection/characterization efficiency or as preprocessing stages of CAD schemes. Apart from the preprocessing methodology used, several parameters entering the CAD system must be tuned in order to achieve high performance. Such parameters are highly correlated with the previously reported preprocessing algorithms. Threshold values of these parameters, are highly correlated with the digitization characteristics of the mammograms, regulate the number and type of the findings, eliminate artifacts, noise or false positive samples. Several types of such parameters have been reported such as the neighborhood size used for the normalization of contrast [31], the block size and the signal-to-noise ratio (SNR) [32], the mean pixel values of the object and its background area [33], the percentage threshold value for pixel selection [34], specific box-rim filters [35] or a combination of them.

In this work, five microcalcification enhancement schemes are used as preprocessing module of a CAD system [36,37]. The first two, the CLAHE and the local range modification (LRM) algorithms are two conventional, well-established methodologies. The other three are sustained on 2-D redundant dyadic wavelet transform (RDWT) utilizing linear stretching and wavelet shrinkage (WSRK) techniques. The utilization of a CAD system as a validation tool for the evaluation of the preprocessing techniques in mammograms is a novel approach. Furthermore, the employment of different enhancement algorithms in the same mammographic datasets provides an additional capability for the evaluation of clinical data. The effect of the enhancement techniques on the detection performance of the CAD system is investigated by means of the following parameters: (a) the percentage value of the most contrasted pixels of the mammogram and (b) the minimum size of the detected object which express a potentially true microcalcification. The system was evaluated using two datasets: the Mammographic Image Analysis Society (MIAS) and the Nijmegen mammographic databases. The evaluation of the enhancement module and parameters tuning is based on ROC analysis.

2. Materials and methods

2.1. Enhancement methodologies

Five representative enhancement methodologies are investigated. The first two are derived from conventional image analysis methodologies, CLAHE and LRM algorithms. The rest are sustained on 2-D RDWT: (a) wavelet linear stretching (WLST) in which, the processed image results by a selective reconstruction using the 2nd and the 3rd level in a four levels decomposition scheme, (b) WSRK which is based on the elimination of the 1st and 4th decomposition levels, (c) wavelet background (WBGK) approximation in which, the preprocessed mammogram result from the 2nd and 3rd levels along with a background level approximation which extracted from the 4th decomposition level.

2.1.1. CLAHE

It is a widely used technique which results in contrast enhancement of medical images [3]. The CLAHE algorithm divides the image into contextual regions and applies histogram equalization to each one of them. It modifies the intensity values of the image employing a nonlinear methodology in order to maximize the contrast for all pixels of the image. This evens out the distribution of used gray values and makes hidden features of the image more visible. However, histogram equalization contains the likelihood of an excessive enhancement of noise, which downgrades the quality of the original image. Based on a desired limit for contrast expansion, a clip limit is obtained equal to 0.5. Each histogram is redistributed so that its height does not go beyond the clip limit. Finally, cumulative distribution functions of the resultant contrast limited histograms are determined for grayscale mapping.

2.1.2. LRM

LRM [38] is a linear stretching approach following formula $y = ax + b$, where y is the enhanced image, x is the original

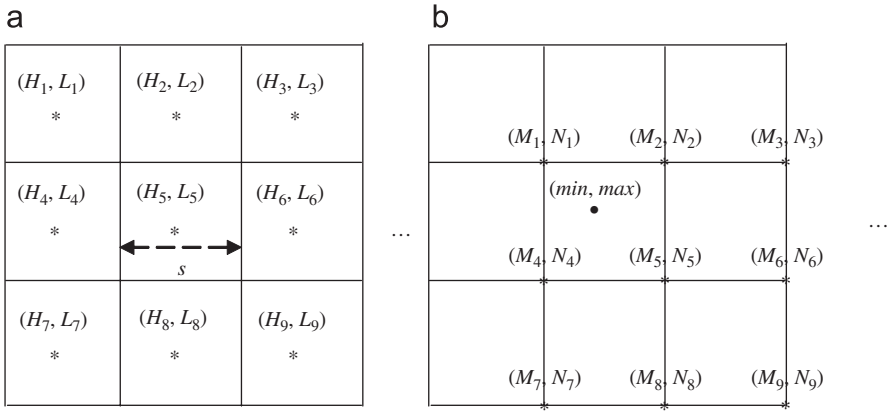

Fig. 1. Estimation of regional maximum and minimum values based on the interpolation of four surrounding grid points. The (H_i, L_i) and (M_i, N_i) are the minimum and maximum grayscale values for each (a) s-size and (b) $2s$-size block.

grayscale image and a, b are parameters depending on the local contrast, which are computed by an interpolation procedure using overlapping image blocks. The LRM algorithm processes twice the whole image. In the first pass, the local parameters are calculated and in the second contrast enhancement is performed. During the first pass, the maximum and the minimum pixel values of non-overlapping 51×51 pixel sized blocks are computed. In the same way, the maximum and the minimum pixel values of half-overlapping blocks are calculated.

In the second pass, an estimation of local maximum and minimum pixel values is achieved by an interpolation of four surrounding grid points (Fig. 1):

$$\max = \left[\frac{s_y}{s} M_4 + \left(\frac{s - s_y}{s}\right) M_1\right]\left(\frac{s - s_x}{s}\right) + \left[\frac{s_y}{s} M_5 + \left(\frac{s - s_y}{s}\right) M_2\right]\frac{s_x}{s}, \quad (1)$$

where s is the size of the block, s_x and s_y are the horizontal and vertical distances of the examined point, respectively, from the M_1 grid point, and M_1, M_2, M_4 and M_5 are the intensity values of the four surrounding grid points.

The output value of each pixel with coordinates $[m, n]$ is calculated by linear stretching:

$$y[m, n] = \frac{L - 1}{(\max - \min)}(x[m, n] - \min), \quad (2)$$

where L is the number of grayscales (image depth), max and min are the margins of the local input grayscale range, respectively. The critical parameter in the LRM algorithm is the local neighborhood length which corresponds to the block size. A size of 51×51 pixels was selected as block size. It is noted that large local maxima or minima develop regions of low contrast around them and sharp differences between two regions of large gray differences result in low-contrast regions.

2.1.3. 2-D RDWT

We use a biorthogonal, over-complete wavelet transform [27], which has been successfully used for mammogram processing [12,28]. The main advantage of the specific wavelet enhancement method is that the local adaptation of parameters of denoising and enhancement transformation functions are applied on the wavelet coefficients. The parameters such as the window size and the contrast limit function do not affect significantly the performance of the technique [39,40]. A selective reconstruction of the processed image composed of only the informative scales, removing coarse or noisy subimages, contributes to improved microcalcification detection. The image is reconstructed using mainly the second and the third decomposition levels. In only the case of WBGK approach the 4th level was partially utilized [41].

Initially, the image is decomposed into a set of subimages using the 2-D RDWT algorithm [27], which provides uniform sampling of the wavelet transform of $f(x, y)$ at any scale large than one, using a particular class of wavelets. For any scale 2^j, the RDWT is defined as a sequence of discrete coefficients:

$$\{S^d_{2^j} f, (W^{1,d}_{2^j} f)_{1 \leqslant j \leqslant J}, (W^{2,d}_{2^j} f)_{1 \leqslant j \leqslant J}\},$$

where

$$W^{1,d}_{2^j} f = (W^1_{2^j} f(n + w, m + w)),$$

$$W^{2,d}_{2^j} f = (W^2_{2^j} f(n + w, m + w)),$$

$$S^d_{2^j} f = (S_{2^j} f(n + w, m + w)). \quad (3)$$

J is the maximum number of the scales of the input image and w is a sampling shift which depends on the choice of wavelets. The wavelet coefficients $(W^{1,d}_{2^j} f)$, $(W^{2,d}_{2^j} f)$ provide the details of the input image at scales $1 \leqslant j \leqslant J$ and the coarse image $S^d_{2^j} f$ is the approximation of the input image at scale 2^j. The relative change of image intensity at each point is expressed by the image gradient magnitude which is highly correlated with the contrast [26]. Thus, contrast enhancement could be achieved changing the gradient magnitude using the wavelet coefficient in each subimage. The magnitude $M_{2^j}(n, m)$ and phase $A_{2^j}(n, m)$ coefficients could be transformed into

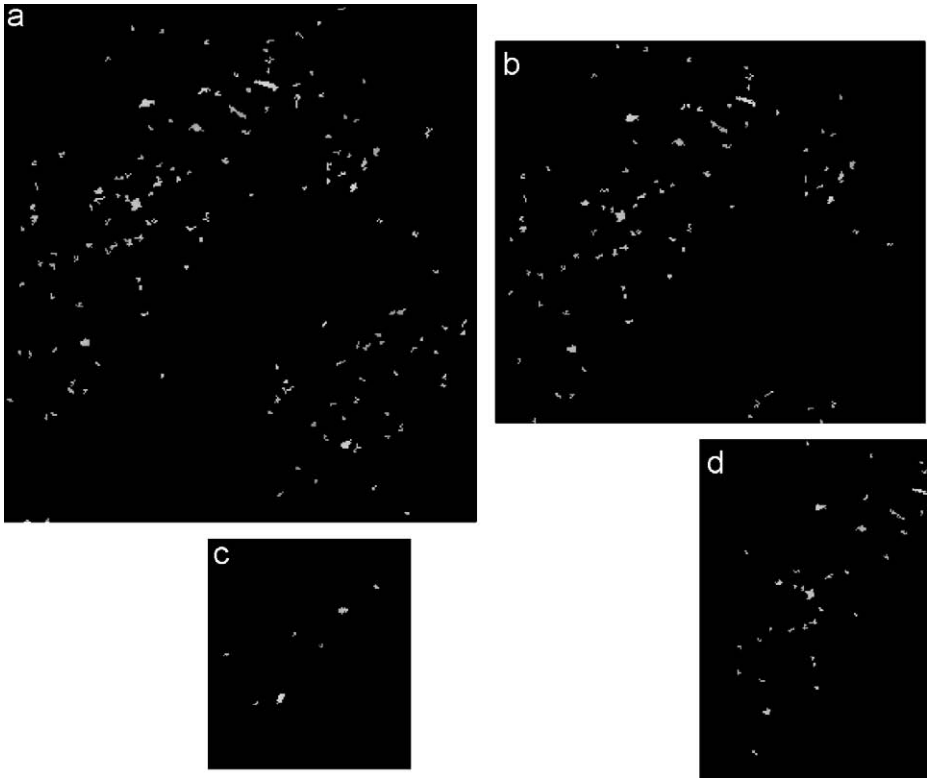

Fig. 2. The selection of different percentage values of most contrasted pixels ((a) 4%, (b) 3%, (c) 2%, (d) 1%) influence significantly the appearance of the microcalcification cluster. Utilizing low percentage values (e.g. 1%) only the large (in area) objects remains as true microcalcifications.

polar co-ordinates:

$$M_{2^j}(n,m) = \sqrt{W^1_{2^j}(n,m) + W^2_{2^j}(n,m)}, \tag{4}$$

$$A_{2^j}(n,m) = \arctan\left(\frac{W^2_{2^j}(n,m)}{W^1_{2^j}(n,m)}\right). \tag{5}$$

2.1.4. RDWT linear stretching (WLST)

Its advantage is the mammographic contrast enhancement by linear or nonlinear mapping of wavelet coefficients [27]. Linear enhancement is obtained using linear stretching of the multiscale gradients:

$$M^{\mathrm{e}}_s(m,n) = k_s M_s(m,n), \tag{6}$$

where $M^{\mathrm{e}}_s(m,n)$ is the enhanced value of gradient magnitude at position (m,n) of the scale s and k_s is a gain parameter ($k_s > 1$), which is applied in each scale enhancing the structures appearing in each level. We have chosen $k_s = 20$ for all scales.

2.1.5. RDWT shrinkage for denoising (WSRK)

It is a method for denoising which sets the wavelet coefficient equal to zero when their magnitude is less than a threshold. We apply either soft thresholding (the magnitude preserves its value) or hard thresholding (the magnitude is set equal to the original value minus the threshold value), i.e.

$$M^d_s(n,m) = \begin{cases} k_s M_s(n,m), & M_s(n,m) > T_s, \\ 0 & \text{otherwise}, \end{cases} \tag{7}$$

where $M^d_s(n,m)$ are the modified magnitude gradients, k_s is the gain parameter and T_s is the threshold at scale s. In our case we have chosen, $k_s = 10$ and $T_s = 60$.

2.1.6. RDWT background approximation (WBGK)

The coarse information which included in the 4th wavelet decomposition level contains data about the sizeable structures in each mammogram. Such structures are the breast tissue area, a possible high density region, and the background area. The enhanced image results from the 2nd and 3rd levels, along with a background level approximation which is extracted from the 4th decomposition level.

2.2. Parameter tuning

The detection of microcalcifications is based on a fully automatic CAD system [36,37]. Two parameters enter the methodology: (a) the percentage of pixels with the highest intensity and local contrast values and (b) the minimum object size. In [36] we have used for the first parameter 5% and for the second 4 pixels. Those values have been obtained after extensive testing. However, those parameters change when a preprocessing module is used.

2.2.1. Percentage of most contrasted pixels

During the tuning process, the percentage of the most intensive and high contrasted pixels is gradually decreased in order

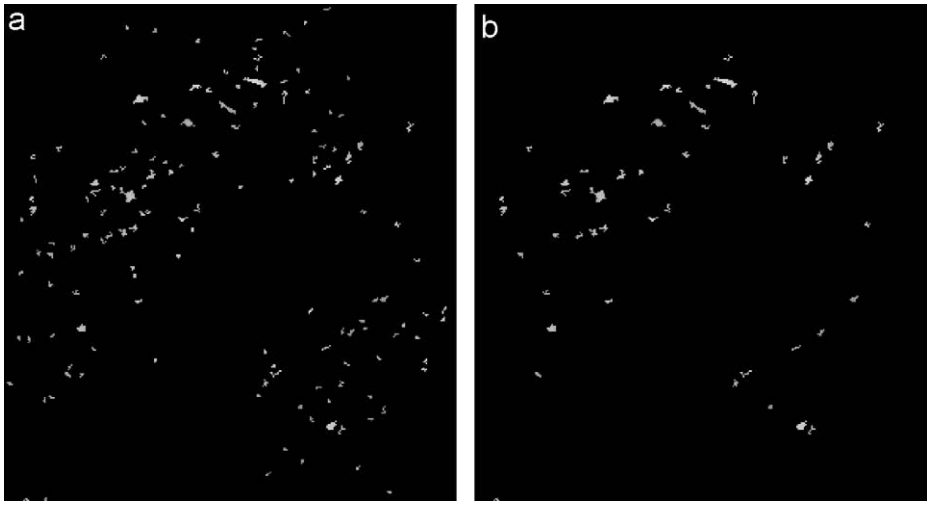

Fig. 3. The effect of the minimum detectable object size in the formulation of the same microcalcification cluster. The segmented objects consist of at least: (a) 4 and (b) 7 pixels.

to enhance the specificity of the detection scheme. Since the central pixel of a microcalcification usually has the highest intensity value, the possible rejection of some boundary pixels does not affect the final object selection. Threshold values of 1%, 2%, 3%, 4% and 5% of the most contrasted pixels were applied in the original (case without the preprocessing module) and the preprocessed images (Fig. 2). The two mammographic databases are analyzed in a similar manner since the effect of parametric tuning must be carried out in both the original and the enhanced images.

As is expected, low values of percentage threshold (e.g. 1%) lead to an increased number of false negative detections which means that at the end of the preprocessing and segmentation modules some real/true microcalcification are lost. The minimization of false negative findings results in an improved performance of the detection system.

2.2.2. Minimum object size

This parameter affects the efficiency of the system in the description of real tiny objects. Thus, its value is very critical in the segmentation module where noise is differentiated from real objects (probable/true microcalcifications—Fig. 3). The performance of the system increases when several false positive findings or tiny objects are removed.

2.3. The classification module (false positive reduction)

The segmentation procedure which is applied in the preprocessed images has been reported in Ref. [36]. However, as in the majority of automated detection schemes, a false positive reduction process is employed in order to minimize the number of false positive findings which decrease the overall performance of the detection system. To classify the segmented objects as true or false samples, several discriminative features were computed and fed into a classification system. In our study, 54 features were calculated for the description of findings. Features related to intensity, shape and textural properties of the cluster or the individual object were extracted. Since the discrimination power of the features vary, a feature selection procedure based on ROC analysis is employed concluding the selection of the most discriminative set which consists of 22 features [36]. The same feature set is utilized in the classification of all the preprocessed images although that the differentiation power of each feature might slightly change after the image enhancement procedure. The classifier that is utilized is a feedforward backpropagation ANN with sigmoid hidden nodes (multilayer perceptron). Two different architectures of the ANNs are utilized, employing one and two hidden layers.

Principal component analysis (PCA) is applied for the elimination of the features that contribute less than 3% to the total variation of dataset. In such a way, PCA transforms the initial size of the feature set from 22 to a 9-D feature space. The training algorithm that is utilized is a quasi-Newton, one-step secant (OSS) algorithm and as a validation procedure is used a two-fold cross-validation methodology. Both datasets are randomly divided into two equal subsets including true and false detections. If the classifier is trained based on the first set, it is tested afterward on the second set and vice versa. The performance is calculated as the average performances of test sets of both folds. However, since the reproducibility of the ANN outcome varies due to the different values of initial conditions, the above process of the ANN testing is repeated 10 times. For each series the maximum value, the average and the standard deviation values of the area under the ROC curve were calculated.

2.4. Characteristics of the microcalcification clusters

As is described in the Introduction, the proposed methodology is developed and applied as part of the preprocessing stage of a CAD system. The design and the implementation of the above system aimed at the detection of microcalcification's clusters that appeared in digitized mammograms.

Microcalcifications are deposits of calcium that can be seen on a mammogram. When many are seen in a cluster, they may indicate an early sight of cancer.

The proposed image enhancement techniques are applied in the microcalcification detection system [36] although microcalcifications are not the only signs that might exist in a cancerous situation (e.g. mammographic masses). Our methodology aims at the improvement of systems' performance in the detection of the small-sized and low-contrast microcalcifications that could be missed or misinterpreted by medical experts. A detailed description of calcifications should include their morphology and their distribution. The CAD system [36] utilized several morphological, intensity and distribution features for the fine description of the type of microcalcifications. Some of the features that are computed from the CAD algorithms are the number of microcalcifications in the cluster, the cluster area, the microcalcifications spreading in cluster as well as the microcalcification compactness, contrast and eccentricity. Part of the feature set is identical to the set of characteristics that is utilized by the experts during their interpretation procedure. Amorphous or indistinct calcifications in a cluster and regional, linear or segmental distributions increase the possibility of malignancy. Additional morphology such as fine pleomorphic calcifications or fine-linear branching suggests filling of the lumen of a duct are irregularly involved in breast cancer.

2.5. Mammographic datasets

For the evaluation of the preprocessing techniques we use the CAD system proposed in [36,37] and the MIAS [42] and the Nijmegen [43] databases. The MIAS database contains 20 mammograms obtained from the medio-lateral oblique view containing 25 annotated microcalcification clusters. Each image is digitized with spatial resolution 50 mm and 8 bit gray depth. A circle enclosing the abnormality indicates the microcalcification cluster. The Nijmegen database contains 40 mammograms of both craniocaudal and oblique views from 21 patients. Digitization has been carried out using an Eikonix 1412 CCD camera with 0.1 mm pixel size and 12 bit gray depth. The size of each image is 2048×2048 pixels. The total number of annotated clusters in the database is 105. It must be noted that the Nijmegen database digitization characteristics are different from the MIAS dataset and, therefore, we resampled the Nijmegen images to change the pixel size from 100 to 50 mm. The resampling technique was actually a magnification process in which each one of the initial pixels was divided to four which have the same intensity value.

3. Results

The original and the five preprocessed images are segmented [36]. For each preprocessing algorithm the performance is reported for various threshold values. Initially, the architecture of the ANN composed of two hidden layers is evaluated. The performance of the detection system utilizing different definition of the minimum object size is reported in Tables 1 and 2, respectively, for the MIAS database. The performance of the system utilizing several values of the parameters and enhancement techniques is shown in Table 3. The highest performance is obtained for the LRM algorithm employing the threshold of 4% for the most contrasted pixels and 7 pixels as the smaller meaningful object. The ROC curve for this case is shown in Fig. 4 ($A_Z = 0.932$). In the case of the Nijmegen database, similar results are obtained, utilizing several threshold which are shown in Tables 4 and 5. Again, the highest performance is achieved for LRM preprocessing employing the same

Table 1
Average A_Z values of the preprocessing techniques for several percentage of the most contrasted pixels values (minimum number of pixels per object: 4)

Percentage of the most contrasted pixels (%)	Enhancement technique					
	CLAHE	LRM	WLST	WSRK	WBGK	Without enhancement
1	0.722	0.763	0.730	0.700	0.75	0.723
2	0.749	0.823	0.782	0.724	0.77	0.75
3	0.844	0.857	0.790	0.770	0.812	0.775
4	0.756	0.878	0.873	0.830	0.845	0.832
5	0.859	0.920	0.901	0.852	0.879	0.866

Table 2
Average A_Z values of preprocessing techniques for several percentage the most contrasted pixels values (minimum number of pixels per object: 7)

Percentage of the most contrasted pixels (%)	Enhancement technique					
	CLAHE	LRM	WLST	WSRK	WBGK	Without enhancement
1	0.670	0.792	0.751	0.742	0.792	0.732
2	0.775	0.815	0.791	0.781	0.833	0.791
3	0.818	0.829	0.763	0.811	0.865	0.818
4	0.837	0.932	0.916	0.841	0.891	0.871
5	0.849	0.926	0.895	0.832	0.881	0.876

Table 3
Detection performance of the CAD system (ROC analysis) utilizing several enhancement techniques and segmentation parameters

Segmentation parameters		Method		Databases	
Area of minimum detectable object (Number of pixels)	Percentage selection (%)	Enhancement	Classification	MIAS-A_Z	Nijmegen-A_Z
4	5	Unenhanced	NN	0.866	0.825
4	5	Unenhanced	Hybrid NN	0.921	0.912
4	5	LRM	Hybrid NN	0.928	0.919
4	5	LRM		0.920	0.903
4	5	CLAHE		0.859	0.814
4	5	WLST		0.901	0.882
4	5	WBGK		0.879	0.874
4	5	WSRK	NN	0.852	0.836
7	4	LRM		0.932	0.915
7	4	CLAHE		0.837	0.802
7	4	WLST		0.916	0.904
7	4	WBGK		0.891	0.887
7	4	WSRK		0.841	0.828

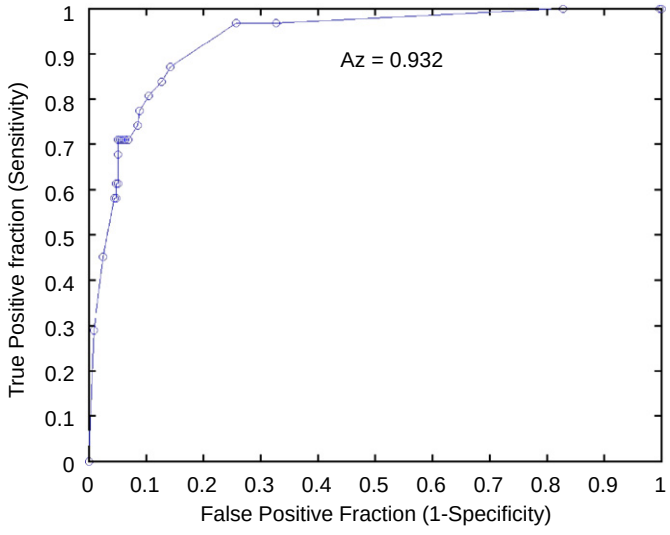

Fig. 4. ROC curve for the LRM enhancement technique for the MIAS database (percentage of the most contrasted pixels: 4% and minimum object size: 7 pixels).

threshold values as in the case of MIAS. The ROC analysis for this case results in $A_Z = 0.915$ as it is shown in Fig. 5.

The average and the STD of the A_Z values for the performance of the system, corresponding to the best values of the parameters, for all preprocessing methods is depicted in Table 6 for both mammographic databases. As it is shown, the LRM technique results in the achievement of the highest average A_Z values with the lowest STD scores. Such behavior emphasizes the superiority of LRM.

The dependence of the performance of the system upon the ANN architecture is also tested utilizing another architecture composed of one hidden layer. The results indicate similar performance as above. The maximum and the average A_Z values decreased for the one hidden layer architecture, while the STD values are reduced improving slightly the confidence of the ANN scheme.

In [36] we have proposed a hybrid system for the detection of microcalcifications. We have again tested all the proposed preprocessing methodologies utilizing the hybrid scheme. However, in the hybrid scheme, the utilization of preprocessing methodologies does not indicate any significant improvement in the detection performance of the system. This is due to the fact that the rules of the hybrid system are designed using characteristics of the original mammogram. The employment of a preprocessing technique changes the importance and the efficiency of the rules and thus does affect the overall performance of the system.

4. Discussion

In this work we have evaluated five preprocessing methodologies, which enhance the mammographic image, which is processed by a CAD system [36]. The use of preprocessing is followed by several stages like segmentation, feature extraction, and an ANN classification to reduce the FP findings. It is understood that the use of a particular preprocessing methodology affects the selection of the parameter values of the CAD system.

The proposed methodology is evaluated using two of the existing standard datasets, the MIAS and the Nijmegen databases. Our results indicate that: (a) The LRM algorithm, in most cases, with the selection of the appropriate values of the tuning parameters, in the highest performance. (b) The ANN architecture only slightly affects the results and the best performance is obtained for LRM for two hidden layers. (c) The second in performance enhancement technique is WLST resulting in $A_Z = 0.916$ and 0.904 for the MIAS and the Nijmegen databases, respectively. (d) The WRSK and the CLAHE techniques result in similar low scores. Those scores are lower than even the achieved performance of the system without the utilization of the preprocessing stage. (e) When a hybrid approach is used for the microcalcification detection, the performance remains the same, even when the best enhancement

Table 4
Average A_Z values of preprocessing techniques for several percentages of most contrasted pixels values (minimum number of pixels per object: 4)

Percentage of the most contrasted pixels (%)	Enhancement technique					
	CLAHE	LRM	WLST	WSRK	WBGK	Without enhancement
1	0.710	0.753	0.713	0.687	0.741	0.721
2	0.741	0.782	0.764	0.713	0.758	0.743
3	0.781	0.841	0.841	0.762	0.804	0.772
4	0.801	0.865	0.862	0.815	0.823	0.803
5	0.834	0.903	0.882	0.836	0.874	0.847

Table 5
Average A_Z values of preprocessing techniques for several percentages of most contrasted pixels values (minimum number of pixels per object: 7)

Percentage of the most contrasted pixels (%)	Enhancement technique					
	CLAHE	LRM	WLST	WSRK	WBGK	Without enhancement
1	0.761	0.781	0.738	0.725	0.782	0.725
2	0.754	0.809	0.784	0.771	0.814	0.789
3	0.798	0.814	0.789	0.783	0.834	0.802
4	0.802	0.915	0.904	0.828	0.887	0.843
5	0.839	0.908	0.892	0.821	0.876	0.838

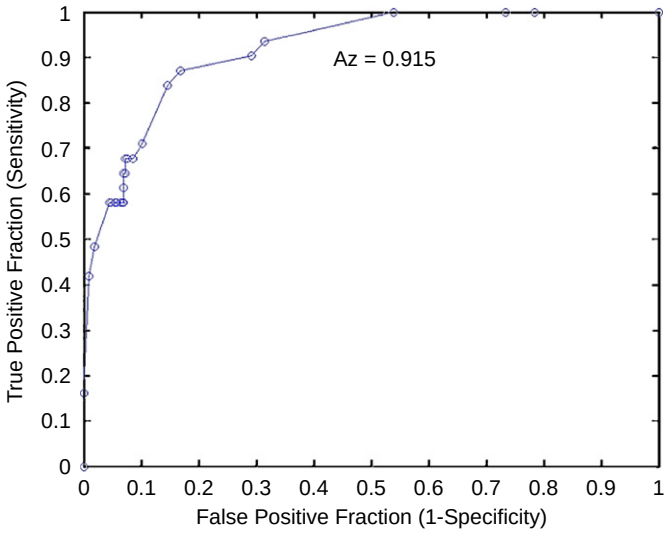

Fig. 5. ROC curve for the LRM enhancement technique for the Nijmegen database (percentage of the most contrasted pixels: 4% and minimum object size: 7 pixels).

technique is used. Such behavior is due to the fact that the extracted rules strongly depend on the processed image.

The performance of the system with the hybrid classification module remains unchanged when preprocessing is used. This is something unexpected. A possible explanation is based on the fluctuation of the image features resulting from an enhancement technique. The features of the neighbor pixels or features of objects are differentiated and the efficiency of the obtained rules is downgraded.

We have selected two parameters that must be tuned in order to achieve better performance. Those are the percentage of the most contrasted pixels and the size of smaller detected microcalcification. The values for those two parameters resulted after extensive experimentation. It is understandable that such an approach is time consuming and not efficient. However, the nature of the problem does not permit derivation of a direct relation of those parameters with the enhancement technique.

In the literature, as far we know, there were no specific references aiming on the evaluation of preprocessing techniques in CAD schemes for microcalcification detection. However, Singh et al. [44] proposed a set of metrics which measure the quality of the image enhancement of mammographic masses in a CAD framework. A single quantitative measure, which arises from the combination of these metrics, suggests the reprocessing technique which results in the highest enhancement effect. On the other hand, there exist several works which address the improvement of radiologist's detection performance utilizing enhancement techniques. Sivaramakrishna et al. [29] assess four enhancement algorithms in order to improve radiologist's interpretation score. An adaptive unsharp masking, a CLAHE, an adaptive-neighborhood contrast enhancement and a wavelet approach were applied on 40 cases containing malignant or benign, microcalcification clusters and masses. The adaptive-neighborhood contrast enhancement algorithm was the most preferred in 49% of the microcalcification interpretations by the radiologists. Wavelet-based approach follows with the preference in 28% and the unenhanced images in 13% of the microcalcification clusters. Hemminger et al. [45] reported an increased detection performance of histogram-based intensity windowing technique compared to CLAHE and unprocessed mammogram in the detection of simulated pathologies. Wavelet contrast enhancement methods reported by Sakellaropoulos et al. [39,40], lead to a significant improvement of local contrast and noise amplification. Direct comparison with the results about the

Table 6
Maximum, average and STD values of A_Z computations in a series of 10 ANN runs, utilizing several initial conditions

Database	Computed values of 10 ANN runs	Enhancement technique					
		CLAHE	LRM	WLST	WSRK	WBGK	Without enhancement
MIAS	Average	0.763	0.881	0.853	0.783	0.822	0.792
	Maximum	0.802	0.915	0.904	0.828	0.887	0.843
	STD	0.034	0.025	0.038	0.027	0.03	0.033
Nijmegen	Average	0.792	0.900	0.840	0.803	0.819	0.831
	Maximum	0.837	0.932	0.916	0.841	0.891	0.875
	STD	0.039	0.023	0.050	0.025	0.034	0.035

efficiency of the enhancement method is not possible, since the CAD systems used are different and none of the researchers tunes parameters of the system.

5. Conclusions

Five enhancement methodologies have been tested aiming at the improvement of the performance of a previously developed CAD system [36] for the detection of microcalcification clusters in digitized mammograms. The employment of the LRM and the WSLT wavelet-based enhancement techniques improved significantly the overall detection performance of the CAD system. Our methodology was evaluated on two of the most well-known mammographic datasets (MIAS and Nijmegen) with satisfactory results. In addition, we addressed tuning of parameters for each of the proposed enhancement techniques and considerable improvement in the system's detection performance has been obtained.

Although, the achieved performance was satisfactory, further studies should be carried out for the utilization of efficient enhancement methodologies aiming at the elimination of falsely detected objects. The employment of wavelet enhancement techniques which would utilize different weights in each level of the image decomposition process can provide a more flexible and probably more effective enhancement in the interpretation of digitized mammograms. Finally, future work will also focus on the construction of enhancement methodologies applied to the classification system that might improve the discrimination between benign and malignant microcalcification clusters.

6. Summary

A computer-aided detection (CAD) system consists of several modules, such as the preprocessing, the segmentation and the reduction of false positive cases. In the preprocessing module, the significant features of the mammogram are enhanced, recovering most of the hidden characteristics and improving image quality. Image enhancement algorithms have been utilized for the improvement of contrast features and the suppression of noise in several types of medical images and more specifically in mammograms.

In this work, the effect of an image enhancement processing stage on parameter tuning of a CAD system for the detection of microcalcifications in mammograms is assessed. Specifically, five (5) image enhancement algorithms were tested: (a) the contrast-limited adaptive histogram equalization (CLAHE), (b) the local range modification (LRM) algorithm, (c) the redundant discrete wavelet (RDW) linear stretching applied on the 2nd and 3rd reconstruction levels, (d) the RDW applied on the 2nd, 3rd and an approximation of 4th reconstruction levels and (e) the RDW shrinkage algorithm applied on the 2nd and 3rd reconstruction levels. The first two are derived from conventional image analysis methodologies based on histogram equalization and linear stretching approaches, respectively. The rest are based on a biorthogonal, over- complete wavelet transform having the advantage that the local adaptation of parameters of denoising and enhancement transformation functions is applied on the wavelet coefficients. A selective reconstruction of the processed image composed of only the informative scales, removing coarse or noisy subimages, contributes to improved microcalcification detection.

Apart from the preprocessing methodology used, several parameters entering the CAD system must be tuned in order to achieve high detection performance. CAD tuning optimization was targeted to the parameters of (a) the percentage of the most contrasted pixels and (b) the size of the minimum detectable object which could satisfactorily represent a microcalcification. In addition, the CAD system was utilized as a validation tool for the evaluation of the preprocessing techniques in mammograms. The treatment of such system as a validation scheme is a novel approach describing a further capability of a CAD system. Furthermore, the employment of different enhancement algorithms in the same mammographic datasets provides an increased potential in the evaluation procedure of clinical mammographic data.

The effect of each preprocessing technique was evaluated by using ROC analysis of CAD system's performance on two mammographic datasets, the Mammographic Image Analysis Society (MIAS) and the Nijmegen databases. The highest area under ROC curve scores (A_Z) in both datasets were achieved for LRM ($A_{Z\mathrm{MIAS}} = 0.932/A_{Z\mathrm{NIJ}} = 0.915$) and the wavelet-based linear stretching ($A_{Z\mathrm{MIAS}} = 0.926/A_{Z\mathrm{NIJ}} = 0.904$) methodology. As for the performance of the rest algorithms, the WRSK and the CLAHE techniques result in similar low scores.

The performance of the system after the utilization of those techniques is quite low obtaining scores lower than the systems' detection score without the employment of enhancement algorithm. In addition, the contribution of the parameters tuning procedure is significant improving considerably the overall detection performance of the CAD system.

As a conclusion, it could be noticed that five enhancement methodologies have been used to improve the performance of a previously designed CAD system aiming at the detection of microcalcification clusters. The contribution of the preprocessing module in the detection ability of the CAD system was definite. In addition, the parametric tuning procedure enhances the detection performance of the CAD system optimizing the segmentation features of the processed mammograms. Future work should be focused on the utilization of more sophisticated enhancement and optimization techniques aiming at further improvement of CAD's detection ability.

Conflict of interest statement

None declared.

Acknowledgements

The Nijmegen database was provided by courtesy of the National Expert and Training Centre for Breast Cancer Screening and the Department of Radiology at the University of Nijmegen, the Netherlands.

References

[1] A. Beghdadi, A.L. Negrate, Contrast enhancement technique based on local detection edges, Comput. Vision Graphics Image Process 46 (1989) 162–174.
[2] A.P. Dhawn, G. Buelloni, R. Gordon, Enhancement of mammographic features by optimal adaptive neighborhood image processing, IEEE Trans. Med. Imaging MI-5 (1986) 8–15.
[3] S.M. Pizer, E.O.P. Amburn, J.D. Austin, Adaptive histogram equalization and its variations, Comput. Vision Graphics Image Process 39 (1987) 355–368.
[4] J.K. Kim, J.M. Park, K.S. Song, H.W. Park, Adaptive mammographic image enhancement using first derivative and local statistics, IEEE Trans. Med. Imaging 16 (1997) 495–502.
[5] R.B. Paranjape, W.M. Morrow, R.M. Rangayyan, Adaptive-neighborhood histogram equalization for image enhancement, Comput. Vision Graphics Image Process 54 (1992) 259–267.
[6] N. Karssemeijer, Adaptive noise equalization and image analysis in mammography, in: Information Processing in Medical Imaging in 13th International Conference, IPMI'93, AZ, USA, 1993, pp. 472–486.
[7] E.D. Pisano, E.B. Cole, B.M. Hemminger, M.J. Yaffe, S.R. Aylward, A.D.A. Maindment, R.E. Johnston, M.B. Williams, L.T. Niklason, E.F. Conant, L.L. Fajardo, D.B. Kopans, M.E. Brown, S.M. Pizer, Image processing algorithms for digital mammography: a pictorial essay, Radiographics 20 (2000) 1479–1491.
[8] H.P. Chan, C.J. Vyborny, H. MacMahon, C.E. Metz, K. Doi, E.A. Sickles, Digital mammography: ROC studies of the effects of pixel size and unsharp-mask filtering on the detection of subtle microcalcifications, Invest. Radiol. 22 (1987) 581–589.
[9] F.Y.M. Lure, P.W. Jones, R.S. Gaborski, Multi-resolution unsharp masking technique for mammogram image enhancement, Proc. SPIE 2710 (1996) 830–839.
[10] W.M. Morrow, R.B. Paranjape, R.M. Rangayyan, Region-based contrast enhancement of mammograms, IEEE Trans. Med. Imaging 11 (1992) 392–406.
[11] R.M. Rangayyan, L. Shen, Y. Shen, Improvement of sensitivity of breast cancer diagnosis with adaptive neighborhood contrast enhancement of mammograms, IEEE Trans. Inf. Technol. Biomed. 1 (1997) 161–170.
[12] A.F. Laine, S. Schuler, J. Fan, W. Huda, Mammographic feature enhancement by multiscale analysis, IEEE Trans. Med. Imaging 13 (4) (1994) 7250–7260.
[13] W. Zhang, H. Yoshida, R.M. Nishikawa, K. Doi, Optimally weighted wavelet transform based on supervised training for detection of microcalcifications in digital mammograms, Med. Phys. 25 (6) (1998) 949–956.
[14] R.N. Strickland, H. Hahn, Wavelet transforms for detecting microcalcifications in mammograms, IEEE Trans. Med. Imaging 15 (2) (1996) 218–229.
[15] W. Qian, L.P. Clarke, B. Zheng, M. Kallergi, R. Clark, Computer assisted diagnosis for digital mammography, IEEE Eng. Med. Biol. Mag. 14 (5) (1995) 561–569.
[16] P. Heinlein, J. Drexl, W. Schneider, Integrated wavelets for enhancement of microcalcifications in digital mammography, IEEE Trans. Med. Imaging 22 (3) (2003) 402–413.
[17] T. Arodz, M. Kurdziel, T.J. Popiela, E.O.D. Sevre, D.A. Yuen, Detection of clustered microcalcifications in small field digital mammography, Comput. Methods Programs Biomed. 8 (1) (2006) 56–65.
[18] H. Li, K.J.U. Liu, S.C.B. Lo, Fractal modeling and segmentation for the enhancement of microcalcifications in digital mammograms, IEEE Trans. Med. Imaging 16 (6) (1997) 785–798.
[19] F. Lefebvre, H. Benali, R. Gilles, E. Kahn, R. Di Paola, A fractal approach to the segmentation of microcalcifications in digital mammograms, Med. Phys. 22 (4) (1995) 381–390.
[20] L. Bocchi, G. Coppini, J. Nori, G. Valli, Detection of single and clustered microcalcifications in mammograms using fractals models and neural networks, Med. Eng. Phys. 26 (2004) 303–312.
[21] H. Sari-Sarref, S. Gleason, R.M. Nishikawa, Front-end data reduction in computer-aided diagnosis of mammograms: a pilot study, Proc. SPIE 3661 (1999) 1535–1543.
[22] J. Jiang, B. Yao, A.M. Wason, Integrating of fuzzy logic and structural tensor towards mammogram contrast enhancement, Comput. Med. Imaging Graph 29 (1) (2005) 83–90.
[23] M.A. Sutton, J. Bezdek, Enhancement and analysis of digital mammograms using fuzzy models, Proc. SPIE 3240 (1997) 179–190.
[24] H. Cheng, Y.M. Luy, R.I. Freimanis, A novel approach to microcalcification detection using fuzzy logic technique, IEEE Trans. Med. Imaging 17 (3) (1998) 442–450.
[25] H.D. Cheng, H. Xu, A novel fuzzy logic approach to mammogram contrast enhancement, Inf. Sci. 148 (2002) 167–184.
[26] A. Laine, J. Fan, W. Yang, Wavelets contrast enhancement of digital mammography, IEEE Eng. Med. Biol. 14 (1995) 536–550.
[27] S. Mallat, S. Zhong, Characterization of signals from multiscale edges, IEEE Trans. Pattern Anal. Mach. Intell. 14 (1992) 710–732.
[28] A. Laine, W. Huda, B.G. Steinbach, J.C. Honeyman, Mammographic image processing using wavelet processing techniques, Eur. Radiol. 5 (1995) 518–523.
[29] R. Sivaramakrishna, N.A. Obuchowski, W.A. Chilcote, G. Cardenosa, K.A. Powell, Comparing the performance of mammographic enhancement algorithms: a preference study, Am. J. Radiol. 175 (2000) 45–51.
[30] L. Costaridou, S. Skiadopoulos, P. Sakellaropoulos, E. Likaki, C.P. Kalogeropoulou, G. Panayiotakis, Evaluating the effect of a wavelet enhancement method in characterization of simulated lesions embedded in dense parenchyma, Eur. Radiol. 15 (8) (2005) 1615–1622.
[31] W.J.H. Veldkamp, N. Karssemeijer, An improved method for detection of microcalcification clusters in digital mammograms, Proc. SPIE 3661 (1999) 512–522.
[32] H.P. Chan, S.C.B. Lo, B. Sahiner, K.L. Lam, M.A. Helvie, Computer-aided detection of mammographic microcalcifications: pattern recognition with an artificial neural network, Med. Phys. 22 (10) (1995) 1555–1567.

[33] B. Zheng, Y. Chang, M. Staiger, W. Good, D. Gur, Computer-aided detection of clustered microcalcifications in digitized mammograms, Acad. Radiol. 2 (1995) 655–662.
[34] H.P. Chan, K. Doi, S. Galhotra, C.J. Vyborny, H. MacMahon, P.M. Jokich, Image feature analysis and computer aided diagnosis in digital radiography. 1. Automated detection of microcalcifications in mammography, Med. Phys. 14 (1987) 538–548.
[35] R.M. Nishikawa, G.E. Mawdsley, A. Fenster, M.J. Yaffe, Scanned projection digital mammography, Med. Phys. 14 (1987) 717–727.
[36] A. Papadopoulos, D.I. Fotiadis, A. Likas, An automatic microcalcification detection system based on a hybrid neural network classifier, Artif. Intell. Med. 25 (2) (2002) 149–167.
[37] A. Papadopoulos, M.E. Plissiti, D.I. Fotiadis, Medical-image processing and analysis for CAD systems, in: L. Costaridou (Ed.), Medical Image Analysis Methods (Electrical Engineering & Applied Signal Processing), CRC Press, Taylor & Francis, Boca Raton, FL, London, 2005, pp. 51–86.
[38] J.D. Fahnestock, R.A. Schowengerdt, Spatially variant contrast enhancement using local range modification, Opt. Eng. 22 (1983) 378–381.
[39] P. Sakellaropoulos, L. Costaridou, G. Panayiotakis, A wavelet-based spatially adaptive method for mammographic contrast enhancement, Phys. Med. Biol. 48 (2003) 787–803.
[40] L. Costaridou, P. Sakellaropoulos, S. Skiadopoulos, G. Panayiotakis, Locally adaptive wavelet contrast enhancement, in: L. Costaridou (Ed.), Medical Image Analysis Methods (Electrical Engineering & Applied Signal Processing), CRC Press, Taylor & Francis, Boca Raton, FL, London, 2005, pp. 225–270.
[41] S. Yu, L. Guan, A CAD system for the automated detection of clustered microcalcifications in digitized mammogram films, IEEE Trans. Med. Imaging 19 (2) (2000) 115–126.
[42] J. Suckling, J. Parker, D. Dance, S. Astley, I. Hutt, C. Boggis, The mammographic images analysis society digital mammogram database, Exerpta Med. 1069 (1994) 375–378.
[43] N. Kassemeijer, Adaptive noise equalization and recognition of microcalcifications in mammography, Int. J. Pattern Recognition Artif. Intell. 7 (1993) 1357–1376.
[44] S. Singh, K. Bovis, An evaluation of contrast enhancement techniques for mammographic breast masses, IEEE Trans. Inf. Technol. Biomed. 9 (1) (2005) 109–119.
[45] B.M. Hemminger, S. Zong, K.E. Muller, C.S. Coffey, M.C. DeLuca, R.E. Johnston, E.D. Pisano, Improving the detection of simulated masses in mammograms through two different image-processing techniques, Acad. Radiol. 8 (9) (2001) 845–855.

Athanassios Papadopoulos received a diploma in Physics from the Department of Physics of the University of Patras, Greece, in 1994 and an M.Sc. degree in Medical Physics from the University of Surrey, UK. He received his Ph.D. from the Department of Medical Physics from the University of Ioannina, Greece. He is also serving as a radiation physicist in the Department of Nuclear Medicine of University Hospital of Ioannina. His research interests include medical image processing, medical decision support, computer-aided detection and diagnosis, machine learning and data mining.

Dimitrios I. Fotiadis was born in Ioannina, Greece, in 1961. He received his Diploma degree in Chemical Engineering from the National Technical University of Athens and the Ph.D. degree in Chemical Engineering from the University of Minnesota, USA. Since 1995, he has been with the Department of Computer Science, University of Ioannina, Greece, where he is currently an Associate Professor. He is the director of the Unit of Medical Technology and Intelligent Information Systems. His research interests include biomedical technology, biomechanics, scientific computing and intelligent information systems.

Lena Costaridou received her diploma in Physics from the Department of Physics of the University of Patras, Greece, an M.Sc. degree in Medical Engineering from the Department of Electrical Engineering and Applied Sciences of the George Washington University, Washington, DC, and in 1997 a Ph.D. degree in Medical Physics from the University of Patras, Greece. She is an Assistant Professor in the Department of Medical Physics, School of Medicine, University of Patras. Her research interests include medical-image processing and analysis applications, especially mammographic image analysis, and evaluation of medical imaging systems and techniques. She is the author or co-author of 40 articles in international peer-reviewed journals and more than 70 international conference papers, as well as the editor of a book on Medical Image Analysis Methods.